CHAPTER ONE

Fundamentals of Radio Communications

The purpose of this chapter is to familiarize the reader with the basic propagation characteristics that describe various wireless communication channels, such as terrestrial, atmospheric, and ionospheric for VHF to the X-band. Well-known standards in wireless communication [1–10] are introduced for the prediction of path losses and fading effects of any radio signal in various communication links, and finally, new possibilities that can be obtained using smart antennas are discussed.

1.1. RADIO COMMUNICATION LINK

Different radio communication links (land, land-to-air, air-to-air) covering different atmospheric and ionospheric conditions, include several components having a plethora of physical principles and processes, with their own independent or correlated working characteristics and operating elements. A simple scheme of such a radio communication link consists of a transmitter (T), a receiver (R), and a propagation channel. The main output characteristics of such a link depend on the conditions of radio propagation in different kinds of environments, as shown in Figure 1.1. According to Reference [6], there are three main independent electronic and electromagnetic design tasks related to this wireless communication network. The first task is the transmitter antenna operation including the specification of the electronic equipment that controls all operations within the transmitter. The second task is to understand, model, and analyze the propagation properties of the channel that connects the transmitting and receiving antennas. The third task concerns the study of all operations related to the receiver.

Radio Propagation and Adaptive Antennas for Wireless Communication Links: Terrestrial, Atmospheric and Ionospheric, by Nathan Blaunstein and Christos Christodoulou

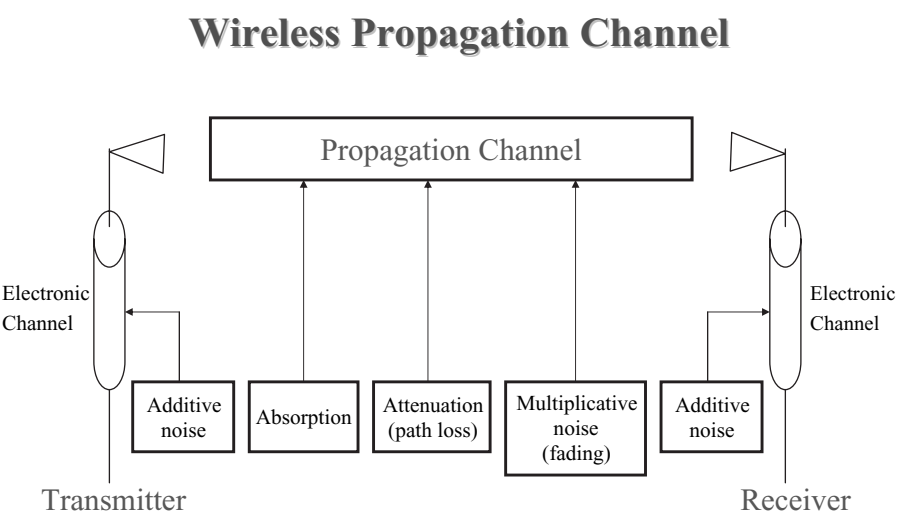

FIGURE 1.1. A wireless communication link scheme.

The propagation channel is influenced by the various obstructions surrounding antennas and the existing environmental conditions. Another important question for a personal receiver (or handheld) antenna is also the influence of the human body on the operating characteristics of the working antenna. The various blocks that comprise a propagation channel are shown in Figure 1.1.

Its main output characteristics depend on the conditions of radio wave propagation in the various operational environments where such wireless communication links are used. Next, we briefly describe the frequency spectrum, used in terrestrial, atmospheric, and ionospheric communications, and we classify some common parameters and characteristics of a radio signal, such as its path loss and fading for various situations, which occur in practice.

1.2. FREQUENCY BAND FOR RADIO COMMUNICATIONS

The *frequency band* is a main characteristic for predicting the effectiveness of radio communication links that we consider here. The optimal frequency band for each propagation channel is determined and limited by the technical requirements of each communication system and by the conditions of radio propagation through each channel. First, consider the spectrum of radio frequencies and their practical use in various communication channels [1–5].

Extremely low and *very low frequencies* (ELF and VLF) are frequencies below 3 kHz and from 3 kHz to 30 kHz, respectively. The VLF band corresponds to waves, which propagate through the wave guide formed by the Earth's surface and the ionosphere at long distances with a low degree of attenuation (0.1–0.5 per 1000 km [1–5]).

Low frequencies (LF) are frequencies from 30 kHz up to 3 MHz. In the 1950s and 1960s they were used for radio communication with ships and aircraft, but since then they are used mainly with broadcasting stations. Because such radio waves propagate along the ground surface, they are called ''surface'' waves [1–5].

High frequencies (HF) are those that are located in the band from 3 MHz up to 30 MHz. Signals in this spectrum propagate by means of reflections caused by the ionospheric layers and are used for communication with aircraft and satellites, and for long-distance land communication using broadcasting stations.

Very high frequencies (VHF) are located in the band from 30 MHz up to 300 MHz. They are usually used for TV communication, in long-range radar systems and radio navigation systems.

Ultra high frequencies (UHF) are those that are located in the band from 300 MHz up to 3 GHz. This frequency band is very effective for wireless microwave links, constructions of cellular systems (fixed and mobile), mobile–satellite communication channels, medium range radars, and other applications.

In recent decades, radio waves with frequencies higher than 3 GHz (C, X, K-bands, up to several hundred gigahertz, which in the literature are referred to as *microwaves*) have begun to be widely used for constructing and performing modern wireless communication channels.

1.3. NOISE IN RADIO COMMUNICATION LINKS

The effectiveness of each radio communication link—land, atmospheric, or ionospheric depends on such parameters, as [5]:

- noise in the transmitter and in the receiver antennas;
- noise within the electronic equipment that communicate with both antennas;
- background and ambient noise (cosmic, atmospheric, artificial man-made, and so forth).

Now let us briefly consider each type of noise, which exists in a complete communication system. In a wireless channel, specifically, the noise sources can be subdivided into *additive* and *multiplicative* effects, as seen in Figure 1.1 [6,7,10].

The *additive noise* arises from noise generated within the receiver itself, such as thermal noise in passive and active elements of the electronic devices, and also from external sources such as atmospheric effects, cosmic radiation, and man-made noise. The clear and simple explanation of the first component of additive noise is that noise is generated within each element of the electronic communication channel due to the random motion of the electrons within the various components of the equipment [5]. According to the theory of thermodynamics, the noise energy can be determined by the average background temperature, T_0, as [1–5]:

$$E_{\mathrm{N}} = k_{\mathrm{B}} T_0 \tag{1.1}$$

where

$$k_B = 1.38 \times 10^{-23}\,\mathrm{W} \times \mathrm{s} \times \mathrm{K}^{-1} \tag{1.2}$$

is Boltzman's constant, and $T_0 = 290\,\mathrm{K} = 17^{\circ}\mathrm{C}$. This energy is uniformly distributed in frequency band and hence it is called "white noise." The total effective noise power at the receiver input is given by the following expression:

$$N_F = k_B T_0 B_W F \tag{1.3}$$

where F is the *noise figure* at the receiver. The noise figure represents any additional noise effects related to the corresponding environment, and it is expressed as:

$$F = 1 + \frac{T_e}{T_0} \tag{1.4}$$

Here T_e is the effective temperature, which accounts all ambient natural (weather, cosmic noise, clouds, rain, and so forth) and man-made (industry, plants, power engine, power stations, and so forth) effects.

The *multiplicative noise* arises from the various processes inside the propagation channel and depends mostly on the directional characteristics of both terminal antennas, on the reflection, absorption, scattering, and diffraction phenomena caused by various natural and artificial obstructions placed between and around the transmitter and the receiver (see Fig. 1.2). Usually, the multiplicative process in the propagation channel is divided into three types: *path loss*, *large-scale* (or *slow fading*), and *short-scale* (or *fast fading*) [7–10]. We describe these three characteristics of the multiplicative noise separately in the following section.

1.4. MAIN PROPAGATION CHARACTERISTICS

In real communication channels, the field that forms the complicated interference picture of received radio waves arrives via several paths simultaneously, forming a multipath situation. Such waves combine vectorially to give an oscillating resultant signal whose variations depend on the distribution of phases among the incoming total signal components. The signal amplitude variations are known as the *fading* effect [1–4,6–10]. Fading is basically a spatial phenomenon, but spatial signal variations are experienced, according to the ergodic theorem [11,12], as temporal variations by a receiver/transmitter moving through the multipath field or due to the motion of scatterers, such as a truck, aircraft, helicopter, satellite, and so on. Thus we can talk here about space-domain and time-domain variations of EM field in different radio environments, as well as in the frequency domain. Hence, if we consider mobile, mobile–aircraft or mobile–satellite communication links, we may observe the effects of random fading in the frequency domain, that is, the

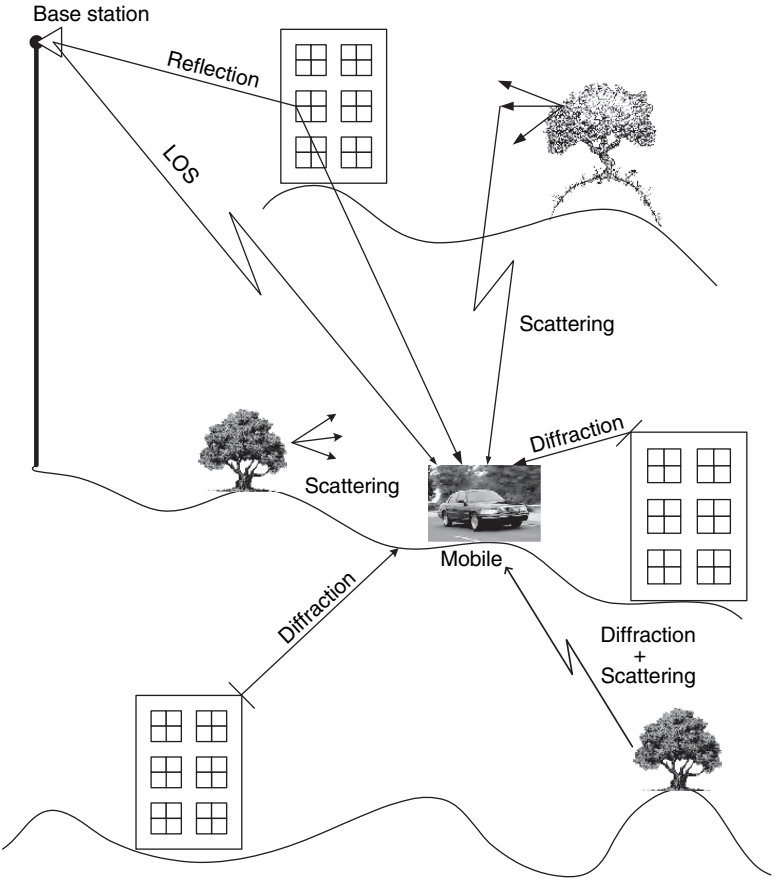

FIGURE 1.2. Multipath effects caused by various natural and artificial obstructions placed between and around the transmitting and the receiving antennas.

complicated interference picture of the received signal caused by receiver/transmitter movements, which is defined as the ''Doppler shift'' effect [1–7,10].

Numerous theoretical and experimental investigations in such conditions have shown that the spatial and temporal variations of signal level have a triple nature [1–7,10]. The first one is the *path loss*, which can be defined as a large-scale smooth decrease in signal strength with distance between two terminals, mainly the transmitter and the receiver. The physical processes that cause these phenomena are the spreading of electromagnetic waves radiated outward in space by the transmitter antenna and the obstructing effects of any natural or man-made objects in the vicinity of the antenna. The spatial and temporal variations of the signal path loss are large and slow, respectively.

Large-scale (in the space domain) or *slow* (in the time domain) fading is the second nature of signal variations and is caused by diffraction from the obstructions

placed along the radio link surrounding the terminal antennas. Sometimes this fading phenomenon is called the *shadowing effect* [6,7,10].

During shadow fading, the signal's slow random variations follow either a Gaussian distribution or a lognormal distribution if the signal fading is expressed in decibels. The spatial scale of these slow variations depends on the dimensions of the obstructions, that is, from several to several tens of meters. The variations of the total EM field describe its structure within the shadow zones and are called *slow-fading* signals.

The third nature of signal variations is the *short-scale* (in the space domain) or *fast* (in the time domain) signal variations, which are caused by the mutual interference of the wave components in the multiray field. The characteristic scale of such waves in the space domain varies from half-wavelength to three-wavelength. Therefore, these signals are usually called *fast-fading* signals.

1.4.1. Path Loss

The path loss is a figure of merit that determines the effectiveness of the propagation channel in different environments. It defines variations of the signal amplitude or field intensity along the propagation trajectory (*path*) from one point to another within the communication channel. In general [1–3, 6–10], the path loss is defined as a logarithmic difference between the amplitude or the intensity (called *power*) at any two different points, $\mathbf{r}_1$ (the transmitter point) and $\mathbf{r}_2$ (the receiver point) along the propagation path in the medium. The path loss, which is denoted by L and is measured in decibels (dB), can be evaluated as follows as [5]:

– for a signal amplitude of $A(\mathbf{r}_j)$ at two points $\mathbf{r}_1$ and $\mathbf{r}_2$ along the propagation path

$$L = 10\log\frac{A^2(\mathbf{r}_2)}{A^2(\mathbf{r}_1)} = 10\log A^2(\mathbf{r}_2) - 10\log A^2(\mathbf{r}_1)$$
$$= 20\log A(\mathbf{r}_2) - 20\log A(\mathbf{r}_1) \quad [\text{dB}] \tag{1.5}$$

– for a signal intensity $J(\mathbf{r}_j)$ at two points $\mathbf{r}_1$ and $\mathbf{r}_2$ along the propagation path

$$L = 10\log\frac{J(\mathbf{r}_2)}{J(\mathbf{r}_1)} = 10\log J(\mathbf{r}_2) - 10\log J(\mathbf{r}_1) \quad [\text{dB}] \tag{1.6}$$

If we assume now $A(\mathbf{r}_1) = 1$ at the transmitter, then

$$L = 20\log A(\mathbf{r}) \quad [\text{dB}] \tag{1.7a}$$

and

$$L = 10\log J(\mathbf{r}) \quad [\text{dB}] \tag{1.7b}$$

For more details about how to measure the path loss, the reader is referred to References [1–3,6–10]. As any signal passing through the propagation channel, passes through the transmitter electronic channel and the electronic channel (see Fig. 1.1), both electronic channels together with the environment introduce additive or white noise into the wireless communication system. Therefore, the second main figure of merit of radio communication channels is the signal-to-noise ratio (SNR or S/N). In decibels this SNR can be written as:

$$\mathrm{SNR} = P_{\mathrm{R}} - N_{\mathrm{R}} \quad [\mathrm{dB}] \tag{1.8}$$

where P_{R} is the signal power at the receiver and N_{R} is the noise power at the receiver.

1.4.2. Characteristics of Multipath Propagation

Here we start with the general description of *slow* and *fast* fading.

Slow Fading. As was mentioned earlier, the *slow* spatial signal variations (expressed in decibels, dB) tend to have a lognormal distribution or a Gaussian distribution (expressed in watts, W) [1–4,6–10]. The probability density function (PDF) of the signal variations with the corresponding standard deviation, averaged within some individual small area or over some specific time period, depends on the nature of the terrain, of the atmospheric and ionospheric conditions. This PDF is given by:

$$\mathrm{PDF}(r) = \frac{1}{\sigma_L\sqrt{2\pi}} \exp\left\{ -\frac{(r-\bar{r})^2}{2\sigma_L} \right\} \tag{1.9}$$

Here $\bar{r} = \langle r \rangle$ is the mean value of the random signal level, r is the value of the received signal strength or voltage envelope, and $\sigma_L = \langle r^2 - \bar{r}^2 \rangle$ is the variance or time-average power ($\langle r \rangle$ indicates the averaging operation of a variable r of the received signal envelope).

Fast Fading. In the case of stationary receiver and transmitter (*static multipath channel*), due to multiple reflections and scattering from various obstructions surrounding the transmitter and receiver, the radio signals travel along different paths of varying lengths, causing such fast deviations of the signal strength (in volts) or power (in watts) at the receiver.

In the case of a *dynamic multipath* situation, either the subscribers' antenna is in movement or the objects surrounding the stationary antennas are moving, so the spatial variations of the resultant signal at the receiver can be seen as temporal variations [11,12]. The signal received by the mobile at any spatial point may consist of a large number of signals having randomly distributed amplitudes, phases, and angles-of-arrival, as well as different time delays. All these features change the relative phase shifts as a function of the spatial location and, finally, cause the signal to fade in the space domain. In a dynamic (mobile) multipath situation, the signal

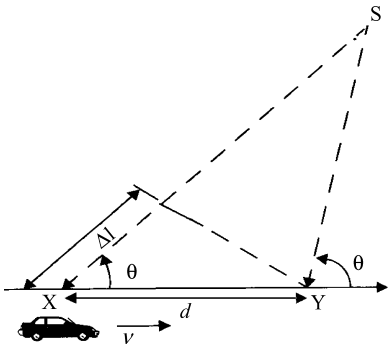

FIGURE 1.3. Geometry of the mobile link for Doppler effect estimation.

fading at the mobile receiver occurs in the time domain. This temporal fading is associated with a shift of frequency radiated by the stationary transmitter. In fact, the time variations, or dynamic changes of the propagation path lengths, are related to the Doppler effect, which is due to relative movements between a stationary base station (BS) and a moving subscriber (MS).

To illustrate the effects of phase change in the time domain due to the Doppler frequency shift (called the Doppler effect [1–4,6–10]), let us consider a mobile moving at a constant velocity v, along the path XY, as shown in Figure 1.3. The difference in path lengths traveled by a signal from source S to the mobile at points X and Y is $\Delta\ell = \ell\cos\theta = v\Delta\cos\theta$, where Δt is the time required for the moving receiver to travel from point X to Y along the path, and θ is the angle between the mobile direction along XY and direction to the source at the current point Y, that is, YS. The phase change of the resultant received signal due to the difference in path lengths is therefore

$$\Delta\Phi = k\Delta\ell = \frac{2\pi}{\lambda}\ell\cos\theta = \frac{2\pi v\Delta t}{\lambda}\cos\theta \tag{1.10}$$

Hence the apparent change in frequency radiated, or Doppler shift, is given by f_D, where

$$f_D = \frac{1}{2\pi}\frac{\Delta\Phi}{\Delta t} = \frac{v}{\lambda}\cos\theta \tag{1.11}$$

It is important to note from Figure 1.3 that the angles θ for points X and Y are the same only when the corresponding lines XS and YS are parallel. Hence, this figure is correct only in the limit when the terminal S is far away from the moving antenna at points X and Y. Many authors have ignored this fact during their geometrical explanation of the Doppler effect [1–4,10]. Because the Doppler shift is related to the mobile velocity and the spatial angle between the direction of mobile motion and the direction of arrival of the signal, it can be positive or negative depending on

whether the mobile receiver is moving toward or away from the transmitter. In fact, from Equation (1.11), if the mobile moves *toward* the direction of arrival of the signal with radiated frequency f_c, then the received frequency is increased, that is the apparent frequency is $f_c + f_D$. When the mobile moves away from the direction of arrival of the signal then the received frequency is decreased, that is the apparent frequency is $f_c - f_D$. The maximum Doppler shift is $f_{Dmax} = v/\lambda$, which, in our futher description will simply be denoted as f_m.

There are many probability distribution functions that can be used to describe the fast fading effects, such as, Rayleigh, Suzuki, Rician, Gamma, Gamma–Gamma, and so on. Because the Rician distribution is very general [1–4,10], as it includes both line-of-sight (LOS) together with scattering and diffraction with non-LOS, we briefly describe it in the following paragraph.

To estimate the contribution of each signal component, at the receiver, due to the dominant (or LOS) and the secondary (or multipath), the Rician parameter K is usually introduced, as a ratio between these components [1–4,10], that is,

$$K = \frac{\text{LOS} - \text{Component power}}{\text{Multipath} - \text{Component power}} \tag{1.12}$$

The Rician PDF distribution of the signal strength or voltage envelope r can be defined as [1–4,10]:

$$\text{PDF}(r) = \frac{r}{\sigma^2}\exp\left\{-\frac{r^2 + A^2}{2\sigma^2}\right\} I_0\left(\frac{Ar}{\sigma^2}\right), \quad \text{for} \quad A > 0, r \geq 0 \tag{1.13}$$

where A denotes the peak strength or voltage of the dominant component envelope, σ is the standard deviation of signal envelope, and $I_0(\cdot)$ is the modified Bessel function of the first kind and zero-order. According to definition (1.12), we can now rewrite the parameter K, which was defined above as the ratio between the dominant and the multipath component power. It is given by

$$K = \frac{A^2}{2\sigma^2} \tag{1.14}$$

Using (1.14), we can rewrite (1.13) as a function of K only, [1–3,10]:

$$\text{PDF}(x) = \frac{r}{\sigma^2}\exp\left\{-\frac{r^2}{2\sigma^2}\right\} \exp(-K) I_0\left(\frac{r}{\sigma}\sqrt{2K}\right) \tag{1.15}$$

For $K = 0$, $\exp(-K) = 1$ and $I_0(0) = 1$, that is, the worst case of the fading channel. The Rayleigh PDF, when there is no LOS signal and is equal to:

$$\text{PDF}(x) = \frac{r}{\sigma^2}\exp\left\{-\frac{r^2}{2\sigma^2}\right\} \tag{1.16}$$

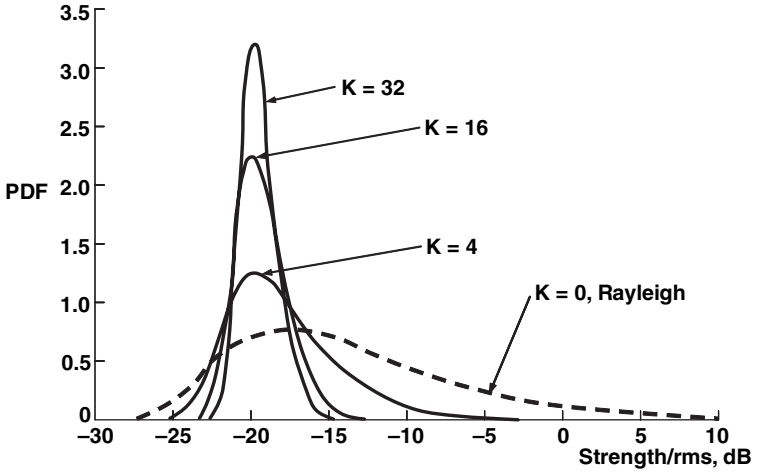

FIGURE 1.4. Rician PDF distribution versus ratio of signal to rms.

Conversely, in a situation of good clearance between two terminals with no multipath components, that is, when $K \to \infty$, the Rician fading approaches a Gaussian one yielding a ''Dirac-delta shaped'' PDF described by formula (1.9) (see Fig. 1.4). We will use these definitions in Chapter 5 for the link budget design inside a terrestrial radio communication system.

1.4.3. Signal Presentation in Wireless Communication Channels

To understand how to describe mathematically multipath fading in communication channels, we need to understand what kinds of signals we ''deal'' with in each channel.

Narrowband (CW) Signals. First of all, we consider a continuous wave CW or *narrowband* signals. A voice-modulated CW signal occupies a very narrow bandwidth surrounding the carrier frequency f_c of the radio frequency (RF) signal (e.g., the carrier), which can be expressed as:

$$x(t) = A(t)\cos[2\pi f_c t + \varphi(t)] \tag{1.17}$$

where $A(t)$ is the signal envelope (i.e., slowly-varied amplitude) and $\varphi(t)$ is its signal phase. For example, for a modulated 1 GHz carrier signal by a wire signal of bandwidth $\Delta f = 2f_m = 8$ KHz, the fractional bandwidth is very narrow, that is, 8×10^3 Hz$/1 \times 10^9$ Hz $= 8 \times 10^{-6}$ or 8×10^{-4}%. Since all information in the signal is contained within the phase and envelope-time variations, an alternative form of a bandpass signal $x(t)$ is introduced [1,2,6–10]:

$$y(t) = A(t)\exp\{j\varphi(t)\} \tag{1.18}$$

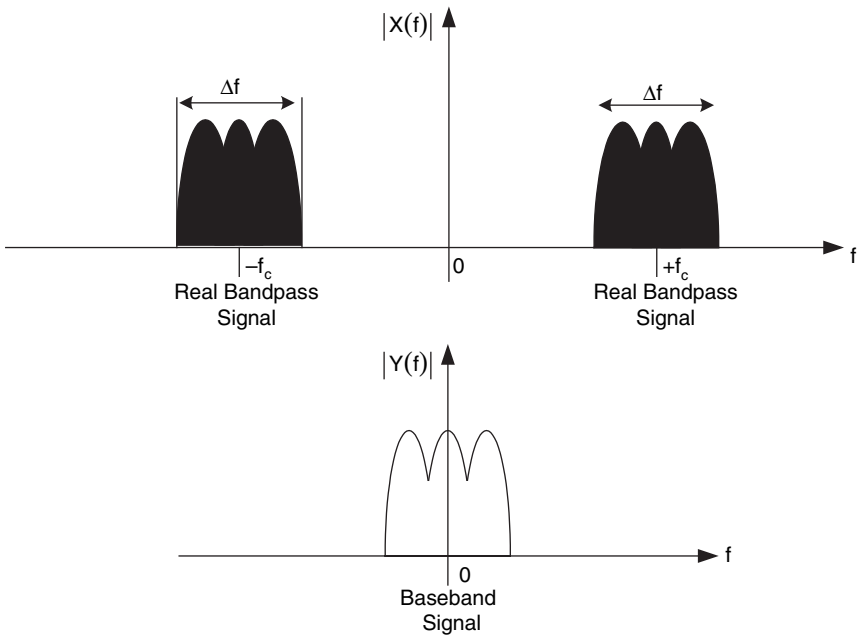

FIGURE 1.5. The signal power presentation of the frequency domain. Bandpath (upper figure) and baseband (lower figure).

which is also called the *complex baseband* representation of $x(t)$. By comparing (1.17) and (1.18), we can see that the relation between the *bandpass* (RF) and the *complex baseband* signals are related by:

$$x(t) = \mathrm{Re}[y(t)\exp(j2\pi f_c t)] \tag{1.19}$$

The relations between these two representations of the narrowband signal in the frequency domain are shown schematically in Figure 1.5. One can see that the complex baseband signal is a frequency shifted version of the bandpass (RF) signal with the same spectral shape, but centered around a zero-frequency instead of the f_c [7]. Here, $X(f)$ and $Y(f)$ are the Fourier transform of $x(t)$ and $y(t)$, respectively and can be presented in the following manner [1,2]:

$$Y(f) = \int_{-\infty}^{\infty} y(t)\mathrm{e}^{-j2\pi ft}\mathrm{d}t = \mathrm{Re}[Y(f)] + j\ \mathrm{Im}[Y(f)] \tag{1.20}$$

and

$$X(f) = \int_{-\infty}^{\infty} x(t)\mathrm{e}^{-j2\pi ft}\mathrm{d}t = \mathrm{Re}[X(f)] + j\ \mathrm{Im}[X(f)] \tag{1.21}$$

Substituting for $x(t)$ in integral (1.21) from (1.19) gives:

$$X(f) = \int_{-\infty}^{\infty} \mathrm{Re}\left[y(t)\mathrm{e}^{j2\pi f_c t}\right]\mathrm{e}^{-j2\pi ft}\mathrm{d}t \tag{1.22}$$

Taking into account that the real part of any arbitrary complex variable w can be presented as:

$$\mathrm{Re}[w] = \frac{1}{2}[w + w^*]$$

where w^* is the complex conjugate, we can rewrite (1.22) in the following form:

$$X(f) = \frac{1}{2}\int_{-\infty}^{\infty} \left[y(t)\mathrm{e}^{j2\pi f_c t} + y^*(t)\mathrm{e}^{-j2\pi f_c t}\right]\mathrm{e}^{-j2\pi ft}\mathrm{d}t \tag{1.23}$$

After comparing expressions (1.20) and (1.23), we get

$$X(f) = \frac{1}{2}[Y(f - f_c) + Y^*(-f - f_c)] \tag{1.24}$$

In other words, the spectrum of the real bandpass signal $x(t)$ can be represented by real part of that for the complex baseband signal $y(t)$ with a shift of $\pm f_c$ along the frequency axis. It is clear that the baseband signal has its frequency content centered around the ''zero'' frequency value.

Now we notice that the mean power of the baseband signal $y(t)$ gives the same result as the mean-square value of the real bandpass (RF) signal $x(t)$, that is,

$$\langle P_y(t)\rangle = \frac{\langle |y(t)|^2\rangle}{2} = \frac{\langle y(t)y^*(t)\rangle}{2} \equiv \langle P_x(t)\rangle \tag{1.25}$$

The complex envelope $y(t)$ of the received narrowband signal can be expressed according to (1.18), within the multipath wireless channel, as a sum of phases of N baseband individual multiray components arriving at the receiver with their corresponding time delay, $\tau_i, i = 0, 1, 2, \ldots, N-1$ [6–10]

$$y(t) = \sum_{i=0}^{N-1} u_i(t) = \sum_{i=0}^{N-1} A_i(t)\exp[j\varphi_i(t, \tau_i)] \tag{1.26}$$

If we assume that during the subscriber movements through the local area of service, the amplitude A_i time variations are small enough, whereas phases φ_i vary greatly

due to changes in propagation distance between the base station and desired subscriber, then there are great random oscillations of the total signal $y(t)$ at the receiver during its movement over a small distance. Since $y(t)$ is the phase sum in (1.26) of the individual multipath components, the instantaneous phases of the multipath components result in large fluctuations, that is, fast fading, in the CW signal. The average received power for such a signal over a local area of service can be presented according to References [1–3,6–10] as:

$$\langle P_{\mathrm{CW}} \rangle \approx \sum_{i=0}^{N-1} \langle A_i^2 \rangle + 2 \sum_{i=0}^{N-1} \sum_{i,j \neq i} \langle A_i A_j \rangle \langle \cos[\varphi_i - \varphi_j] \rangle \tag{1.27}$$

Wideband (Pulse) Signals. The typical *wideband* or *impulse* signal passing through the multipath communication channel is shown schematically in Figure 1.6a according to [1–4]. If we divide the time-delay axis into equal segments, usually called bins, then there will be a number of received signals, in the form of vectors or delta functions. Each bin corresponds to a different path whose time-of-arrival is within the bin duration, as depicted in Figure 1.6b. In this case

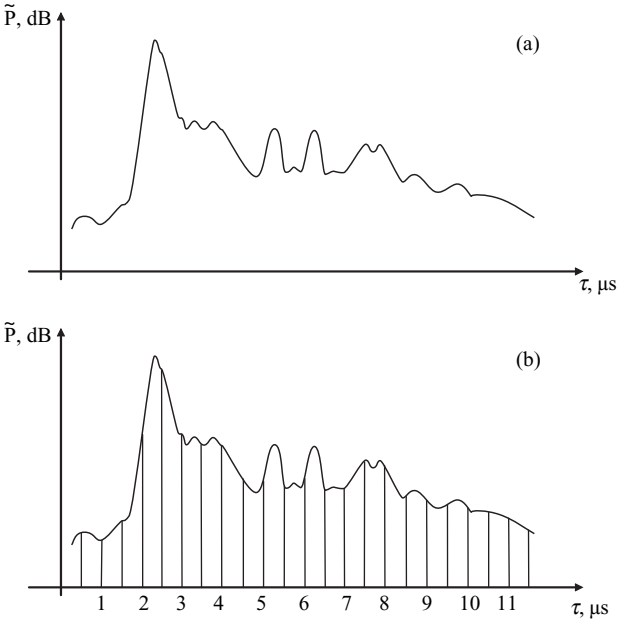

FIGURE 1.6. (a) A typical impulse signal passing through a multipath communication channel according to [1–4]. (b) The use of binds, as vectors, for the impulse signal with spreading.

the time varying discrete-time impulse response can be expressed as:

$$h(t,\tau) = \left\{ \sum_{i=0}^{N-1} A_i(t,\tau) \exp[-j2\pi f_c \tau_i(t)] \delta(\tau - \tau_i(t)) \right\} \exp[-j\varphi(t,\tau)] \tag{1.28}$$

If the channel impulse response is assumed to be time invariant, or is at least stationary over a short-time interval or over a small-scale displacement of the receiver/transmitter, then the impulse response (1.28) reduces to

$$h(t,\tau) = \sum_{i=0}^{N-1} A_i(\tau) \exp[-j\theta_i] \delta(\tau - \tau_i) \tag{1.29}$$

where $\theta_i = 2\pi f_c \tau_i + \varphi(\tau)$. If so, the received power delay profile for a wideband or pulsed signal averaged over a small area can be presented simply as a sum of the powers of the individual multipath components, where each component has a random amplitude and phase at any time, that is,

$$\langle P_{\text{pulse}} \rangle = \left\langle \sum_{i=0}^{N-1} \{A_i(\tau) | \exp[-j\theta_i]|\}^2 \right\rangle \approx \sum_{i=0}^{N-1} \langle A_i^2 \rangle \tag{1.30}$$

The received power of the wideband or pulse signal does not fluctuate significantly when the subscriber moves within a local area, because in practice, the amplitudes of the individual multipath components do not change widely in a local area of service.

Comparison between small-scale presentations of the average power of the narrowband (CW) and wideband (pulse) signals that is, (1.27) and (1.30), shows that when $\langle A_i A_j \rangle = 0$ or/and $\langle \cos[\varphi_i - \varphi_j] \rangle = 0$, the average power for CW signal and that for pulse are equivalent. This can occur when either the path amplitudes are uncorrelated, that is, each multipath component is independent after multiple reflections, diffractions, and scattering from obstructions surrounding both the receiver and the transmitter or the base station and the subscriber antenna. It can also occur when multipath phases are independently and uniformly distributed over the range of $\lfloor 0, 2\pi \rfloor$. This property is correct for UHF/X-waveband when the multipath components traverse differential radio paths having hundreds of wavelengths [6–10].

1.4.4. Parameters of the Multipath Communication Channel

So the question that is remains to be answered which kind of fading occurs in a given wireless channel.

Time Dispersion Parameters. First some important parameters for a wideband (pulse) signal passing through a wireless channel, can be determined, for a certain threshold level X (in dB) of the channel under consideration, from the signal

power delay profile, such as mean excess delay, rms delay spread and excess delay spread.

The *mean excess delay* is the first moment of the power delay profile of the pulse signal and is defined as:

$$\langle \tau \rangle = \frac{\sum_{i=0}^{N-1} A_i^2 \tau_i}{\sum_{i=0}^{N-1} A_i^2} = \frac{\sum_{i=0}^{N-1} P(\tau_i)\tau_i}{\sum_{i=0}^{N-1} P(\tau_i)} \tag{1.31}$$

The *rms delay spread* is the square root of the second central moment of the power delay profile and is defined as

$$\sigma_\tau = \sqrt{\langle \tau^2 \rangle - \langle \tau \rangle^2} \tag{1.32}$$

where

$$\langle \tau^2 \rangle = \frac{\sum_{i=0}^{N-1} A_i^2 \tau_i^2}{\sum_{i=0}^{N-1} A_i^2} = \frac{\sum_{i=0}^{N-1} P(\tau_i)\tau_i^2}{\sum_{i=0}^{N-1} P(\tau_i)} \tag{1.33}$$

These delays are measured relative to the first detectable signal arriving at the receiver at $\tau_0 = 0$. We must note that these parameters are defined from a single power delay profile, which was obtained after temporal or local (small-scale) spatial averaging of measured impulse response of the channel [1–3,7–10].

Coherence Bandwidth. The power delay profile in the time domain and the power spectral response in the frequency domain are related through the Fourier transform. Hence, to describe a multipath channel in full, both the delay spread parameters in the time domain, and the *coherence bandwidth* in the frequency domain are used. As mentioned earlier the coherence bandwidth is the statistical measure of the frequency range over which the channel is considered ''flat.'' In other words, this is a frequency range over which two frequency signals are strongly amplitude correlated. This parameter, actually, describes the time dispersive nature of the channel in a small-scale (local) area. Depending on the degree of amplitude correlation of two frequency separated signals, there are different definitions for this parameter.

The first definition is the *coherence bandwidth*, B_c, which describes a bandwidth over which the frequency correlation function is above 0.9 or 90%, and it is given by:

$$B_c \approx 0.02\sigma_\tau^{-1} \tag{1.34}$$

The second definition is the *coherence bandwidth*, B_c, which describes a bandwidth over which the frequency correlation function is above 0.5 or 50%, or:

$$B_c \approx 0.2\sigma_\tau^{-1} \tag{1.35}$$

There is not any single exact relationship between coherence bandwidth and rms delay spread, and equations (1.34) and (1.35) are only approximate equations [1–6,7–10].

Doppler Spread and Coherence Time. To obtain information about the time varying nature of the channel caused by movements, from either the transmitter/receiver or scatterers located around them, new parameters, such as the *Doppler spread* and the *coherence time*, are usually introduced to describe the time variation phenomena of the channel in a small-scale region. The Doppler spread B_D is defined as a range of frequencies over which the received Doppler spectrum is essentially nonzero. It shows the spectral spreading caused by the time rate of change of the mobile radio channel due to the relative motions of vehicles (and scatterers around them) with respect to the base station. According to [1–4,7–10], the Doppler spread B_D depends on the Doppler shift f_D and on the angle α between the direction of motion of any vehicle and the direction of arrival of the reflected and/or scattered waves (see Fig. 1.3). If we deal with the complex baseband signal presentation, then we can introduce the following criterion: If the baseband signal bandwidth is greater than the Doppler spread B_D, the effects of Doppler shift are negligible at the receiver.

Coherence time T_c is the time domain dual of Doppler spread, and it is used to characterize the time varying nature of the frequency dispersiveness of the channel in time coordinates. The relationship between these two-channel characteristics is:

$$T_c \approx \frac{1}{f_m} = \frac{\lambda}{v} \tag{1.36}$$

We can also define the coherence time according to [1–4,7–10] as the time duration over which two multipath components of receiving signal have a strong potential for amplitude correlation. One can also define the coherence time as the time over which the correlation function of two various signals in the time domain is above 0.5 (or 50%). Then according to [7,10] we get

$$T_c \approx \frac{9}{16\pi f_m} = \frac{9\lambda}{16\pi v} = 0.18\frac{\lambda}{v} \tag{1.37}$$

This definition is approximate and can be improved for modern digital communication channels by combining Equations (1.36) and (1.37) as the geometric mean between the two, this yields

$$T_c \approx \frac{0.423}{f_m} = 0.423\frac{\lambda}{v} \tag{1.38}$$

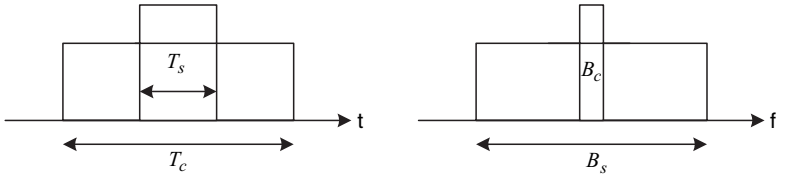

FIGURE 1.7. Comparison between signal and channel parameters.

The definition of coherence time implies that two signals arriving at the receiver with a time separation greater than T_c are affected differently by the channel.

1.4.5. Types of Fading in Multipath Communication Channels

Let us now summarize the effects of fading, which may occur in static or dynamic multipath communication channels.

Static Channel. In this case multipath fading is purely spatial and leads to constructive or destructive interference at various points in space, at any given instant in time, depending on the relative phases of the arriving signals. Furthermore, fading in the frequency domain does not change because the two antennas are stationary. The signal parameters, such as the signal bandwidth, B_s, the time of duration, T_s, with respect to the coherent time, B_c, and the coherent bandwidth, T_c, of the channel are shown in Figure 1.7. There are two types of fading that occur in the static channels:

A. *Flat slow fading* (FSF) (see Fig. 1.8), where the following relations between signal parameters of the signal and a channel are valid [7–10]:

$$T_c \gg T_s; \quad 0 \cong B_D \ll B_s; \quad \sigma_\tau \ll T_s; \quad B_c \sim \frac{0.02}{\sigma_\tau} \gg B_s \tag{1.39}$$

Here all harmonics of the total signal are coherent.

B. *Flat fast fading* (FFF) (see Fig. 1.9), where the following relations between the parameters of a channel and the signal are valid [7–10]:

$$T_c \gg T_s; \quad 0 \cong B_D \ll B_s; \quad \sigma_\tau \leqslant T_s; \quad B_c \ll B_s \tag{1.40}$$

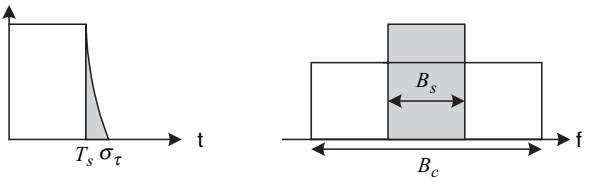

FIGURE 1.8. Relations between parameters for flat slow fading.

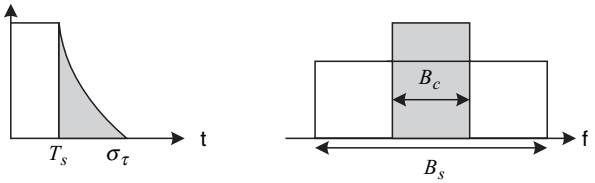

FIGURE 1.9. Relations between parameters for flat fast fading.

Dynamic Channel. There are two different types of fading also that occur in a dynamic (mobile) channel:

A. *Frequency selective fast fading* (FSFF) (see Fig. 1.10), when fast fading depends on the frequency. In this case following relations between the parameters of a channel and the signal are valid [7–10]:

$$T_c \ll T_s; \quad B_D \gg B_s; \quad \sigma_\tau \gg T_s; \quad B_c \ll B_s \tag{1.41}$$

B. *Frequency selective slow fading* (FSSF) (see Fig. 1.11), when slow fading depends on the frequency. Therefore, the following relations between the parameters of a channel and the signal are valid [7–10]:

$$T_c > T_s; \quad B_D < B_s; \quad \sigma_\tau < T_s; \quad B_c \gg B_s \tag{1.42}$$

Using these relationships between the parameters of the signal and of a channel, we can a priori define the type of fading which may occur in a wireless communication link (see Fig. 1.12).

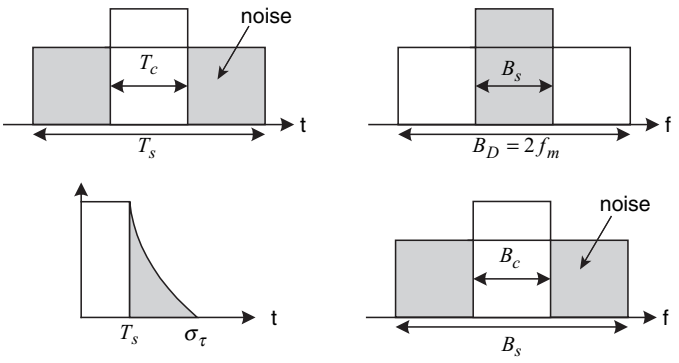

FIGURE 1.10. Relations between parameters for frequency selective fast fading.

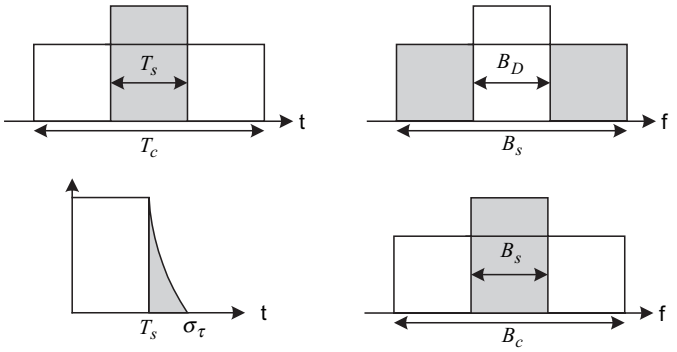

FIGURE 1.11. Relations between parameters for frequency selective slow fading.

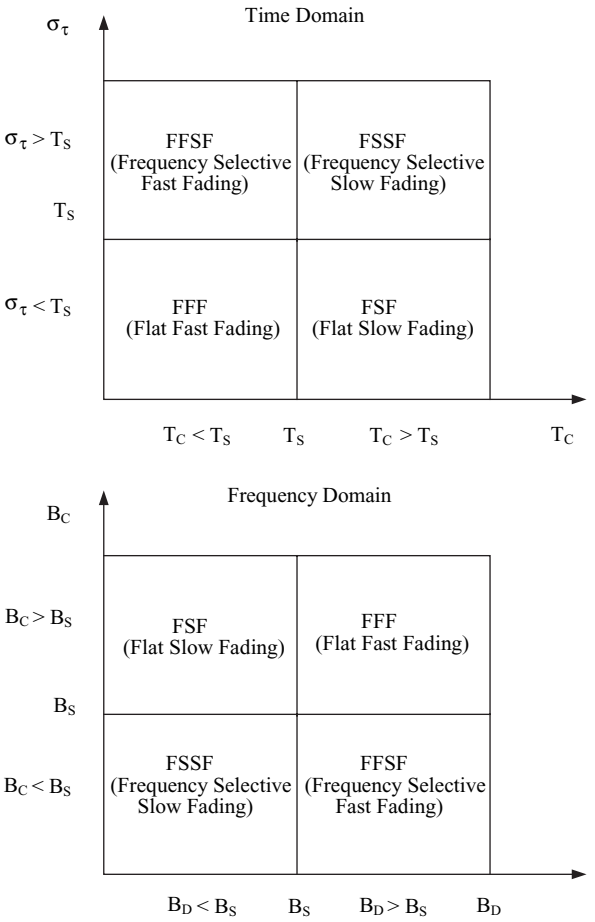

FIGURE 1.12. Common picture of different kinds of fading, depending on the relations between the signal and the channel main parameters.

1.5. PROBLEMS IN ADAPTIVE ANTENNAS APPLICATION

The main problem with land communication links is estimating the ratio between the coherent and multipath components of the total signal. That is, the Ricean parameter K, to predict the effects of multiplicative noise in the channel of each subscriber located in different conditions in the terrestrial environment. This is shown in Figure 1.13 for various subscribers numbered by $i = 1, 2, 3, \ldots$.

However, even a detailed prediction of the radio propagation situation for each subscriber cannot completely resolve all issues of effective service and increase quality of data stream sent to each user. For this purpose, in future generations of wireless systems, adaptive or smart antenna systems are employed to reduce interference and decrease bit error rate (BER). This topic will be covered in detail in Chapter 8. We present schematically the concept of adaptive (smart) antennas in Figure 1.14.

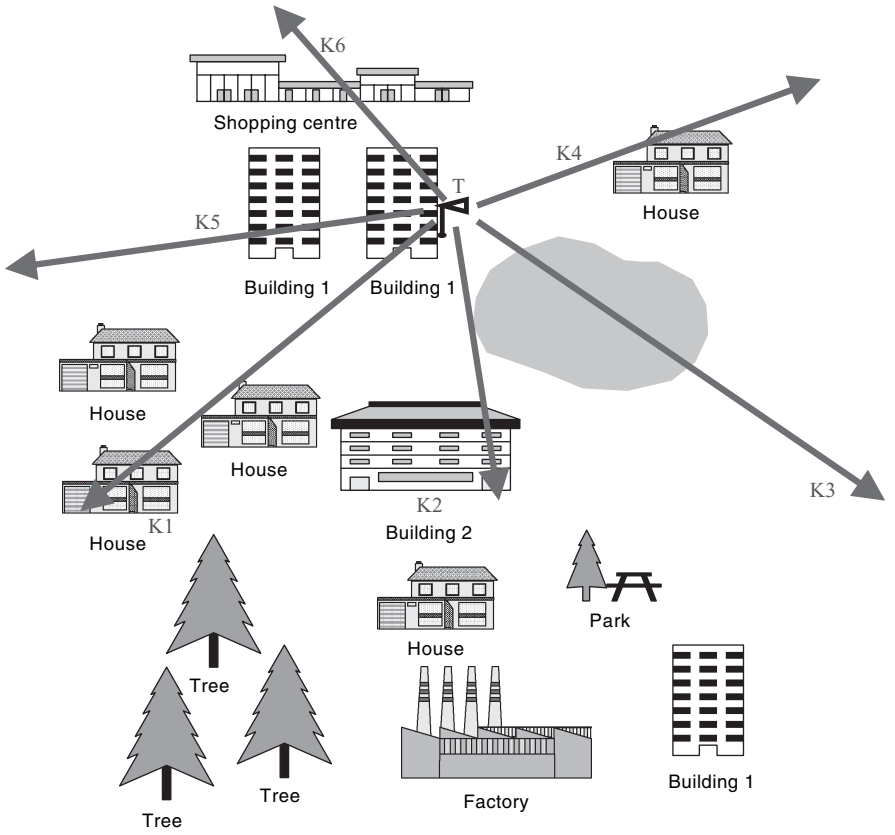

FIGURE 1.13. Scheme of various scenarios in urban communication channel.

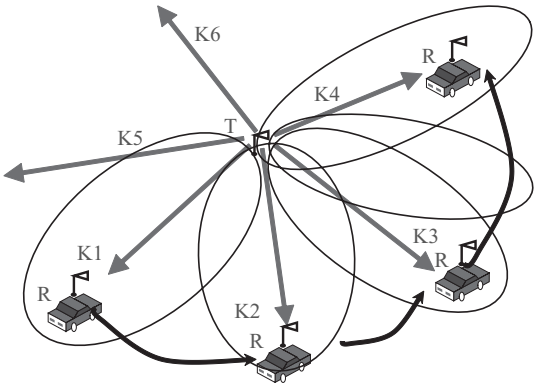

FIGURE 1.14. A scheme for using adaptive antennas for each user located in different conditions in a service area.

Even with smart antennas (see Chapter 8), we cannot totally cancel the effects of the environment, especially in urban areas, due to the spread of the antenna beam (see Fig. 1.14). Chapters 5 and 10 will focus on terrain effects where a thorough analysis of these effects on the design of wireless system will be presented.

BIBLIOGRAPHY

[1] Jakes, W. C., *Microwave Mobile Communications*, New York, John Wiley and Son, 1974.

[2] Steele, R., *Mobile Radio Communication*, IEEE Press, 1992.

[3] Stuber, G. L., *Principles of Mobile Communications*, Boston-London, Kluwer Academic Publishers, 1996.

[4] Lee, W. Y. C., *Mobile Cellular Telecommunications Systems*, McGraw Hill, New York, 1989.

[5] Blaunstein, N., *Radio Propagation in Cellular Networks*. Artech Houses, Boston-London, 1999.

[6] Blaunstein, N., and J. B. Andersen, *Multipath Phenomena in Cellular Networks*, Artech Houses, Boston-London, 2002.

[7] Saunders, S. R., *Antennas and Propagation for Wireless Communication Systems*, John Wiley & Sons, New York, 1999.

[8] Bertoni, H. L., *Radio Propagation for Modern Wireless Systems*, Prentice Hall PTR, New Jersey, 2000.

[9] Blaunstein, N., Chapter 12*, Wireless Communication Systems*, *Hanbook of Engineering Electromagnetics*, Edited by Rajeev Bansal, Marcel Dekker, NY, 2004.

[10] Rappaport, T. S., *Wireless Communications*, New York, Prentice Hall PTR, 1996.

[11] Leon-Garcia, A., *Probability and Random Processes for Electrical Engineering*, New York: Addison-Wesley Publishing Company, 1994.

[12] Stark, H., and Woods J. W., *Probability, Random Processes, and Estimation Theory for Engineers*, New Jersey, Prentice Hall, 1994.